



Inferring the size scales of planetary systems using resolved debris discs

J. P. Marshall^{1,2}, N. Pawellek^{3,4}, G. M. Kennedy^{5,6}, P. Scicluna¹, and A. V. Krivov⁷

¹ Academia Sinica, Institute of Astronomy and Astrophysics, 11F Astronomy-Mathematics Building, NTU/AS campus, No. 1, Section 4, Roosevelt Rd., Taipei 10617, Taiwan

² Computational Engineering and Science Research Centre, University of Southern Queensland, Toowoomba, QLD 4350, Australia

³ Max-Planck-Institut für Astronomie, Königstuhl 17, 69117 Heidelberg, Germany

⁴ Konkoly Observatory, Research Centre for Astronomy and Earth Sciences, Hungarian Academy of Sciences, P.O. Box 67, H-1525 Budapest, Hungary

⁵ Department of Physics, University of Warwick, Gibbet Hill Road, Coventry CV4 7AL, UK

⁶ Centre for Exoplanets and Habitability, University of Warwick, Gibbet Hill Road, Coventry CV4 7AL, UK

⁷ Astrophysikalisches Institut und Universitätssternwarte, Friedrich-Schiller-Universität Jena, Schillergässchen 2-3, 07745 Jena, Germany

Abstract. Circumstellar debris discs are tenuous remnant rings of icy and rocky material left over from planet(esimal) formation processes around their host stars. Possible relationships between stellar luminosity and disc parameters have been examined. Based on analysis of a sample of 39 spatially resolved debris discs at infrared wavelengths by Herschel, a trend between stellar luminosities (L_*) and the ratio of the discs' resolved radii (R_d) to blackbody radii (R_{bb}) was noted. We have examined a larger sample of resolved debris discs from archival far-infrared Herschel observations in order to determine the fidelity of that trend. We further examine whether the inferred extents of these discs are consistent with self-stirring models or may be indicative of dynamical perturbation by a planetary companion. Disc radii were determined by fitting the source brightness profiles with simple annular disc models convolved with a PSF. We obtain good agreement between the resolved extent of debris discs as measured at millimetre wavelengths and the estimates based on L_* and R_d/R_{bb} at far-infrared wavelengths, suggesting that the measured trend is a fair, albeit imperfect, predictor of actual disc extent. In future work we will apply this revised relationship to the larger sample of unresolved debris discs in an attempt to identify systems that exhibit evidence of stirring by a planetary companion.

Key words. Stars: circumstellar matter – stars: planetary systems

1. Introduction

Debris discs around main sequence stars are the visible remnants of planet formation processes. The dust that constitutes the visible

component of these structures is continually replenished by collisions between larger, unseen planetesimals (asteroids and comets) and is typically detected as excess emission, above that predicted for the host star, at infrared

wavelengths (Wyatt 2008; Matthews et al. 2014). Typically, the excess thermal emission from dust is observed at mid- and/or far-infrared wavelengths (e.g. Eiroa et al. 2013; Montesinos et al. 2016; Sibthorpe et al. 2018; Thureau et al. 2014), but an increasing number of systems have been resolved at sub-millimetre wavelengths (e.g. Matrà et al. 2018; Marshall et al. 2018). These dusty systems are analogous to the Solar system with its Asteroid Belt and Edgeworth-Kuiper Belt (Nesvorný et al. 2010; Vitense et al. 2012), albeit often larger in scale, and more massive.

Most debris discs are spatially unresolved, such that a degeneracy exists between the radial extent of the disc and the temperature of the dust grains in modelling of these sources (e.g. Krivov et al. 2008). In the absence of other information, an estimate of a disc’s radial extent could be made assuming that its constituent dust grains radiated as blackbodies, such that the radial extent of the disc, i.e. its blackbody radius (R_{bb}), could be accurately inferred from the dust temperature (Backman & Paresce 1993; Wyatt 2008). Since dust grains are imperfect absorbers or emitters of radiation, they will be warmer than the blackbody temperature for a given radius from the star. The true disc radius (R_{d}) will therefore always be larger than the blackbody radius.

Analysis of various *Herschel*-resolved debris discs has revealed that those discs around FG-type stars are more extended than would be inferred from the dust temperature ($R_{\text{d}}/R_{\text{bb}}$ up to 10 for Sun-like stars, Marshall et al. 2011; Wyatt et al. 2012; Marshall et al. 2014a) whilst discs around A-type stars more closely matched the extent predicted from the dust temperature (i.e. $R_{\text{d}}/R_{\text{bb}} \sim 1-2$, Booth et al. 2013; Morales et al. 2013). The results of Pawellek et al. (2014) and Pawellek & Krivov (2015) revealed that a dust composition containing ice was favoured in fitting the $\Gamma-L_{\star}$ relation, which would be expected from material at 10s au around the host star and is supported by independent studies (Morales et al. 2016). The addition of five K-type stars to the *Herschel*-resolved discs sample of Pawellek & Krivov (2015) in Pawellek (2017) resulted in a better radius determination for the discs around

lower luminosity stars at the cost of favouring no particular dust composition.

The presence of debris discs and giant exoplanets has been found to be correlated, confirming debris discs as a signpost of planetary systems (Matthews et al. 2014). Further studies identified tentative correlations between the presence of discs and low-mass planets around low metallicity host stars (Wyatt et al. 2012; Marshall et al. 2014b), and in the presence of discs around stars with wide-orbiting Jovian exoplanets (Maldonado et al. 2012; Meshkat et al. 2017). Larger samples have not confirmed these initial findings, potentially due to the sample selection criteria, weak upper limits on the presence of debris from infrared photometry, and poor sensitivity to wide-orbiting and/or low-mass exoplanets due to time baseline/radial velocity sensitivity to low-mass planets (Moro-Martín et al. 2015; Wittenmyer & Marshall 2015).

Modelling of the radial extent of young disc host stars resolved by *Herschel* has identified that several exhibit properties compatible with the presence of a perturbing planet rather than disc self-stirring (e.g. Moór et al. 2015; Vican et al. 2016; Dodson-Robinson et al. 2016). Obtaining a reliable measure of the radii of debris discs that can be applied to unresolved discs that will be found by future missions, e.g. *Spica*, is of critical importance in being able to interpret the scale of these planetary systems and determine the influence of any potential planets on the distribution of debris in such systems.

The remainder of the paper is presented as follows. In Section 2, we present the modelling approach used to determine disc radii and dust temperatures. In Section 3, we compare the results of our analysis of the expanded sample with disc radii as observed at sub-mm wavelengths, and predictions from self- and planet-stirring disc models. These results are discussed in the context of recent work on disc radius–stellar luminosity trends and disc stirring models in Section 4. Finally, in Section 5, we give our conclusions.

2. Modelling

We obtain far-infrared images of the 67 resolved discs analysed here from the *Herschel* Science Archive. These are complemented by comprehensive spectral energy distributions compiled from infrared to millimetre wavelength photometry. The stellar component of each system is fitted using a suitable NEXTGEN photosphere model.

The spatial distribution of the extended emission in the *Herschel*/PACS images is modelled using a single Gaussian ring plus an unresolved stellar component. The Gaussian ring is described by a peak radius (R_{peak}), fractional width (ΔR), inclination (i), position angle (ϕ), and flux (f_{ring}). The unresolved stellar component has a flux equivalent to the appropriate photospheric emission and is assumed to lie at the centre of the disc. A model is convolved with the instrument PSF, which is then subtracted from the observed image and the properties of the residuals within the region of the image where the $s/n \geq 3\sigma$ are calculated. The best fitting disc parameters are determined in a Bayesian framework using 10,000 realisations (100 walkers, 100 steps) to sample the parameter space with the Python code `EMCEE` (Foreman-Mackey et al. 2013).

The best fit disc architecture for each system is used as fixed input to a radiative transfer dust emission model that has the minimum grain size (a_{min}), size distribution exponent (q), and mass (in dust up to 1 mm) as free parameters. For this step, we again use `EMCEE` to explore parameter space with 10,000 realisations, comparing the calculated emission models to the observed photometry for wavelengths $> 30 \mu\text{m}$, so as to avoid the presence of warm dust components in biasing the minimum grain size toward smaller values. We assume the dust grains to be compact spheres of astronomical silicate, given the lack of compositional preference in Pawellek & Krivov (2015).

Having determined a_{min} for a given disc, we can then calculate R_d/R_{bb} for each disc taking the dust temperature from a modified blackbody fit to the spectral energy distribution and comparing it to the expected dust temperature at the observed radial location for grains

of the minimum size inferred from the radiative transfer modelling.

3. Results

3.1. Fidelity of the far-infrared relationship

We first fit the ensemble of resolved discs from Pawellek et al. (2014) with with a function of the same form as reported in Pawellek & Krivov (2015), i.e. $\Gamma = \alpha L_{\star}^{\beta}$, where $\Gamma = R_d/R_{\text{bb}}$. In their work, the constants α and β adopt different values depending on the assumed composition of dust grains.

Here we adopt a Bayesian approach to estimate the maximum likelihood and confidence intervals for parameters α and β . We assume there is an additional intrinsic scatter component to the data, ϵ , such that

$$\Gamma = \alpha L_{\star}^{\beta} + \epsilon \quad (1)$$

With this model assumption, we adopt uniform priors on the values of free parameters α and β in the ranges $[1,10]$ and $[-1,0]$, respectively. The free parameter ϵ is assumed to have a Gaussian distribution with a standard deviation dependent on Γ . The likelihood function is taken from Hogg et al. (2010), having recast the fitting process into that of the form

$$\Gamma = \log_{10}(\alpha) + \beta \log_{10}(L_{\star}) + \epsilon \quad (2)$$

We sample the posterior probability distribution of the parameter space using a Markov Chain Monte Carlo approach with the code `EMCEE`. We sample the distributions with 1,000 walkers over 1,000 steps; the initial locations of the walkers are randomised in parameter space centred on the least-squares fit. From this process we obtain values of $\alpha = 5.64^{+0.65}_{-0.57}$ and $\beta = -0.387^{+0.100}_{-0.064}$, where the parameter and its associated uncertainties are the 50⁺³⁴₋₃₄ percentiles of the distributions. The expanded sample of discs examined in this work is presented in Fig. 1 alongside the original sample of Pawellek et al. (2014), whilst the MCMC fitting results are shown in Fig. 2. These values are entirely consistent with the previously obtained best-fit estimates through least-squares

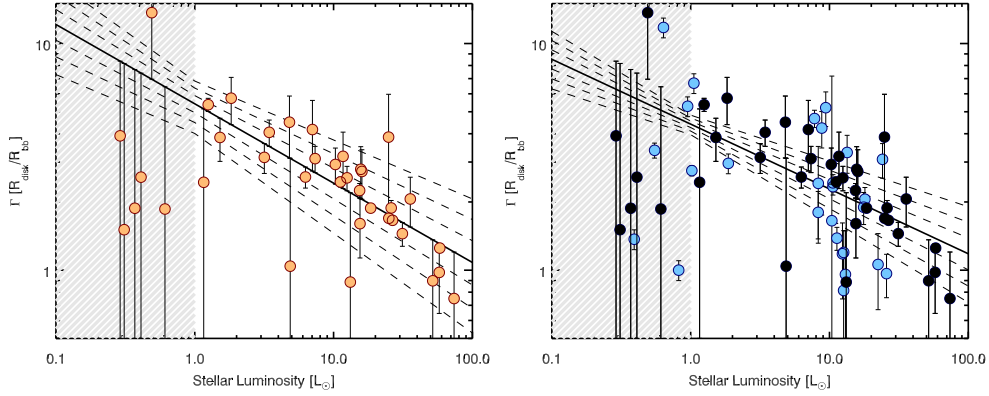


Fig. 1. Plot showing Γ , the ratio of a disc’s resolved extent to its blackbody radius (i.e. R_d/R_{bb}), to the stellar luminosity. Left: The original Pawellek et al. (2014) sample as red data points with the best-fit relationship determined by Pawellek & Krivov (2015) over-plotted for reference (solid black line, dotted lines are $\pm 1-3\sigma$ uncertainties). The grey shading denotes the region where the relationship breaks down due to the absence of a blowout radius for dust grains around stars of sub-Solar luminosity. Right: The revised $\Gamma-L_\star$ relationship and uncertainties based on a least-squares fit to the expanded sample from this work. The original sample from Pawellek et al. (2014) are denoted by the black data points, additional discs are denoted by blue data points.

minimisation (i.e. $\alpha = 5.42 \pm 0.47$, $\beta = -0.35 \pm 0.03$, Pawellek & Krivov 2015), with larger uncertainties representative of the intrinsic scatter.

3.2. Comparison with mm-resolved discs

We now consider the reliability of radial extents derived from the $\Gamma-L_\star$ relationship. In Fig. 3, we present a comparison of the disc radii determined from ALMA or SMA observations against their radii as determined from the dust temperature and stellar luminosity with our scaling relationship. The sub-sample of millimetre-resolved discs comprises 26 stars (Matrà et al. 2018), and spans a range in stellar luminosities consistent with the wider sample (1 to $30 L_\odot$). It should therefore be representative of any systematic trends in the quality of the radii derived from our modelling.

A comparison of the millimetre-resolved discs in Matrà et al. (2018) and the calculated radii based on our $\Gamma-L_\star$ relationship reveals general good agreement between the two,

as seen in Fig. 3. As expected, the predictive capacity of the $\Gamma-L_\star$ relationship completely breaks down below $1 L_\odot$. However, there are several notable exceptions to the consistency between the observations and predictions around higher luminosity stars. Most notably, the predicted radii for HD 15115, HD 111520, HD 8907, and HD 377 are larger than the observed radii by ~ 2 . This has previously been noted from analysis of the original sample of 34 resolved discs, e.g. in the case of HD 104860 (Pawellek & Krivov 2015). In the case of HD 15115 and HD 111520 the mismatch might be explained as the result of the discs being highly asymmetric, which is inconsistent with the tacit assumption that there is a single characteristic dust temperature (and therefore disc radius). However, both HD 8907 and HD 377 have been resolved as having well confined annular discs, such that the assumptions inherent to predicting their disc radii hold true. Given that the mismatch becomes more apparent as the stellar luminosity decreases, it might well be the over-prediction of disc radii is the effect of the natural diversity of dust grain properties present in discs; for higher

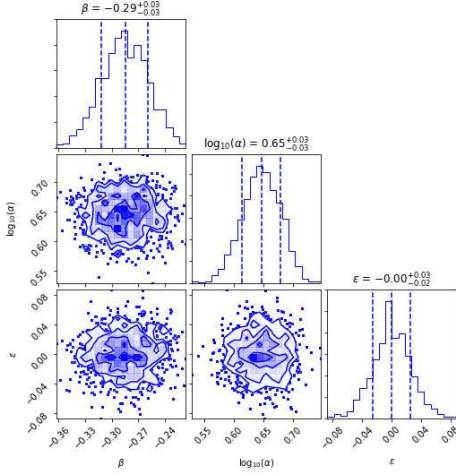


Fig. 2. Marginalised posterior probability distributions of the parameters $\log \alpha$, β , and ϵ . Histograms are the probability distribution of a single parameter marginalised over the other two. Contour plots illustrate the probability distributions of pairs of parameters marginalised over the third. Contours represent the confidence intervals bounding 68, 95.5, and 99.73 per cent of the distributions.

luminosity stars the diversity (and impact) of dust grain properties is masked by their acting more like blackbodies overall.

4. Discussion

Overall, there is good general agreement between the observed and predicted radii, within the admittedly large uncertainties afforded to the latter. We see that all (8/8) of the disc radii are consistent (overlapping) for stars with $L_\star > 10 L_\odot$, but this declines with stellar luminosity. For stars $3L_\odot \leq L_\star \leq 10L_\odot$ it is 5/6 and $1L_\odot \leq L_\star \leq 3L_\odot$ it is 3/7. This is perhaps due to the low number of resolved discs around stars at 1 to $10 L_\odot$, such that their contribution to the best-fit relationship is under-weighted. Below $1 L_\odot$, 2/5 disc estimates overlap, despite the null predictive power of the relationship there. Where disagreement is present, the tendency is for the inferred radius to be an over-estimate compared to the observed disc radius (7/9); in the remaining two cases, HD 146897 and HD 146181, the disc radii are underestimated.

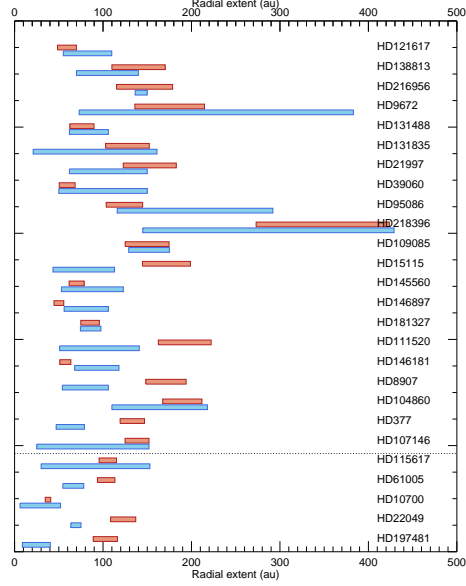


Fig. 3. Plot of radii for resolved debris discs taken from Matrà et al. (2018) (in blue) compared to estimates from the revised Γ - L_\star relationship presented here (in red). Systems are arranged in decreasing stellar luminosity from top to bottom, with those below the horizontal dashed line having $L_\star < L_\odot$, where the Γ - L_\star relationship has no predictive power.

A more detailed discussion of these general trends, along with the peculiarities of individual systems, is deferred to a future work.

5. Conclusions

We have presented an analysis of far-infrared resolved debris discs in order to further refine a relationship between Γ and L_\star determined from previous studies of a small sample of such systems. We omitted systems from the analysis that have been shown to be influenced by a planetary companion, or are otherwise identified as anomalous. We found that the trend determined in this work is still consistent with the relationship previously obtained using the smaller sample, after omitting potentially biasing sources from the pool of resolved discs.

Comparison of the inferred extent from this analysis and the measured extent at millimetre wavelengths (Matrà et al. 2018) demonstrated good agreement between the two, sup-

porting the continued application of this trend in estimation of disc extent for unresolved sources. There is some evidence for the disc radii around lower luminosity stars to be over-predicted. The addition of more resolved debris discs around stars with luminosities $< 10 L_{\odot}$ to the sample will be an invaluable contribution to better determination of the $\Gamma-L_{\star}$ trend, which is currently heavily biased toward discs around higher luminosity stars.

Acknowledgements. This research has been supported by the Ministry of Science and Technology of Taiwan under grants MOST104-2628-M-001-004-MY3 and MOST107-2119-M-001-031-MY3, and Academia Sinica under grant AS-IA-106-M03. This research has made use of the SIMBAD database, operated at CDS, Strasbourg, France. This research has made use of NASA's Astrophysics Data System. This research made use of the Python packages ASTROPY (The Astropy Collaboration et al. 2018), MATPLOTLIB (Hunter 2007), EMCEE (Foreman-Mackey et al. 2013), and CORNER (Foreman-Mackey 2016).

References

- Backman, D. E. & Paresce, F. 1993, in *Protostars and Planets III*, ed. E. H. Levy & J. I. Lunine (Univ. Arizona Press, Tucson), 1253
- Booth, M., Kennedy, G., Sibthorpe, B., et al. 2013, *MNRAS*, 428, 1263
- Dodson-Robinson, S. E., Su, K. Y. L., Bryden, G., Harvey, P., & Green, J. D. 2016, *ApJ*, 833, 183
- Eiroa, C., Marshall, J. P., Mora, A., et al. 2013, *A&A*, 555, A11
- Foreman-Mackey, D. 2016, *The Journal of Open Source Software*, 24
- Foreman-Mackey, D., Hogg, D. W., Lang, D., & Goodman, J. 2013, *PASP*, 125, 306
- Hogg, D. W., Bovy, J., & Lang, D. 2010, *ArXiv e-prints*, arXiv:1008.4686
- Hunter, J. D. 2007, *Computing in Science and Engineering*, 9, 90
- Krivov, A. V., Müller, S., Löhne, T., & Mutschke, H. 2008, *ApJ*, 687, 608
- Maldonado, J., Eiroa, C., Villaver, E., Montesinos, B., & Mora, A. 2012, *A&A*, 541, A40
- Marshall, J. P., Kirchschrager, F., Ertel, S., et al. 2014a, *A&A*, 570, A114
- Marshall, J. P., Löhne, T., Montesinos, B., et al. 2011, *A&A*, 529, A117
- Marshall, J. P., Milli, J., Choquet, É., et al. 2018, *ApJ*, 869, 10
- Marshall, J. P., Moro-Martín, A., Eiroa, C., et al. 2014b, *A&A*, 565, A15
- Matrà, L., Marino, S., Kennedy, G. M., et al. 2018, *ApJ*, 859, 72
- Matthews, B. C., et al. 2014, in *Protostars and Planets VI*, ed. H. Beuther et al. (Univ. Arizona Press, Tucson), 521
- Meshkat, T., Mawet, D., Bryan, M. L., et al. 2017, *AJ*, 154, 245
- Montesinos, B., Eiroa, C., Krivov, A. V., et al. 2016, *A&A*, 593, A51
- Moór, A., Kóspál, Á., Ábrahám, P., et al. 2015, *MNRAS*, 447, 577
- Morales, F. Y., et al. 2013, *ApJ*, 776, 111
- Morales, F. Y., et al. 2016, *ApJ*, 831, 97
- Moro-Martín, A., Marshall, J. P., Kennedy, G., et al. 2015, *ApJ*, 801, 143
- Nesvorný, D., Jenniskens, P., Levison, H. F., et al. 2010, *ApJ*, 713, 816
- Pawellek, N. 2017, PhD thesis, Jena, dissertation, Friedrich-Schiller-Universität Jena, 2016
- Pawellek, N. & Krivov, A. V. 2015, *MNRAS*, 454, 3207
- Pawellek, N., Krivov, A. V., Marshall, J. P., et al. 2014, *ApJ*, 792, 65
- Sibthorpe, B., Kennedy, G. M., Wyatt, M. C., et al. 2018, *MNRAS*, 475, 3046
- The Astropy Collaboration, Price-Whelan, A. M., Sipőcz, B. M., et al. 2018, *ArXiv e-prints*, arXiv:1801.02634
- Thureau, N. D., Greaves, J. S., Matthews, B. C., et al. 2014, *MNRAS*, 445, 2558
- Vican, L., Schneider, A., Bryden, G., et al. 2016, *ApJ*, 833, 263
- Vitense, C., et al. 2012, *A&A*, 540, A30
- Wittenmyer, R. A. & Marshall, J. P. 2015, *AJ*, 149, 86
- Wyatt, M. C. 2008, *ARA&A*, 46, 339
- Wyatt, M. C., Kennedy, G., Sibthorpe, B., et al. 2012, *MNRAS*, 424, 1206